CHAPTER 6
Measurement and analysis of polarisation dispersion in optical fibres

In this chapter, detailed experimental results are presented describing the polarisation properties of different types of fibres, such as S-SMF, DSF, spun DSF, DEDF and EDF, with and without twist. The results are used:

(a) For confirmation that the theory developed in Chapter 5 correctly describes the DGD evolution versus twist. This is applicable to cabled fibres where a small amount of twist is often unavoidable during fibre fabrication, cabling and deployment.

(b) To investigate the initial DGD of these fibres, and to show that there exists an ideal elastic twist for each fibre which minimises the initial DGD.

(c) In trying to understand if elastic twisted fibre can reduce the fibre sensitivity to external pressure, as external stress can be induced during cabling and may lead to a higher PMD in some fibres.

(d) For analysis of spun fibre with sinusoidal spin, which, in parallel with simulation results, helped to develop an empirical equation from which the minimum effective spin needed can be calculated, in order to obtain sufficient DGD reduction.

(e) The investigation of DGD in fibres for the forward-backward direction with reflection helps to understand if a fibre with reflection behaves in a reciprocal manner.

From the list (Table 6.1) of the measured short length DGD values the range of the cabled fibre PMD, as under field conditions, has been estimated for some of these fibres by using typical mode coupling lengths. If the fibre PMD is known, the bandwidth limitation due to PMD can then be estimated.

The structure of this chapter is as follows. Section 6.1 describes the measurement and simulation results for the DGD versus external applied twist for different kind of fibres, giving experimental confirmation for the theory developed in Chapter 5. At the beginning of the section a table of the measured fibres is given detailing the fibre manufacturers and measured intrinsic DGD values, giving a comprehensive overview of all the measurement results. The DGD of fibre versus external applied pressure, similar to that likely for cabled fibre, has also been measured. This is especially interesting for spun fibres where cabling may be the dominant source of PMD. Section 6.2 considers the DGD versus twist of a fibre measured in the forward-backward direction using Fresnel reflection at the far end of the fibre. This not only allowed the finding of the zero twist position with access to only one end of the fibre, but also demonstrated the cancellation of the circular polarisation dispersion as due to the reciprocity of the fibre. Section 6.3 treats spun fibre with a sinusoidal spin which has only recently emerged onto the market. By comparing the measured DGD versus external applied twist for samples of spun fibres to numerical simulation, as introduced in Section 5.4, an approximate equation for the necessary effective spin as a function of the initial linear birefringence could be found, so that the fibre exhibits minimal overall DGD. Section 6.4 considers the error in the measured DGD values. The PMD on shipping bobbins has been measured for some of the fibres and is compared with the corresponding short length DGD values. This allowed the calculation of the mode coupling length of spooled fibres, which was then extended to the expected mode coupling length in cabled fibres, using information available from external sources about the cabling effect on fibre PMD. Section 6.5 examines the bandwidth limitations due to PMD in non-regenerated optical systems.

6.1 Measurement of DGD as a function of twist in different fibres

6.1.1 The Experimental set-up

To test the validity of the theoretical model derived in Chapter 5 the DGD of different fibre samples, as a function of twist, has been measured using the Hewlett Packard (HP) PMD measurement equipment, using Jones matrix eigenanalysis [137] to calculate the DGD of the fibre around the centre wavelength $\lambda = 1.55$ μm. The HP PMD measurement equipment has a specified minimum resolution of 1 fs, and is composed of an external tunable laser source HP 8168A, with a tuning range from 1470 to 1580 nm, and a 3-state linear polarisation generator contained within the polarimeter unit (HP-8509A).

The experimental set-up for twisting the fibre is shown in Figure 6.1. The ends of the fibre under test were connected to the tunable wavelength source via the linear polarisation state generator and to the polarimeter. The fibre under test was folded in half over bobbins, with a diameter of either 32 cm or 15 cm at the far end, and each half was allowed to hang in a catenary, with a maximum length of 60 metres (see figures in Appendix D). This ensured an even distribution of the twist applied by rotating the fibre ends with an accuracy of 10º.

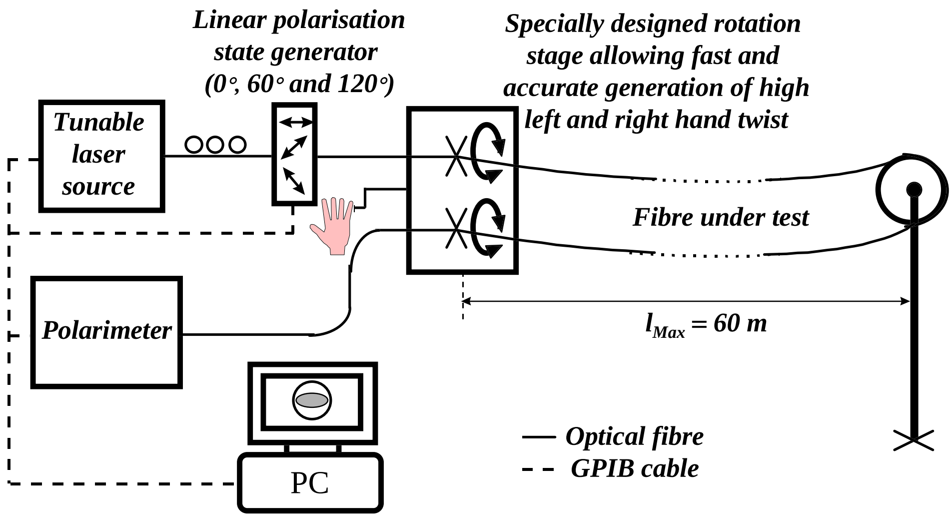

Figure 6.1 Set-up for twisting the fibre and measuring of the PMD. See also Appendix D for twisting set-up as used in the tunnel.

6.1.2 The measured fibres and some other measurement aspects

6.1.2.1 List of measured fibres and measurement results

The fibres which have been measured are S-SMFs, DSFs, DSFs Spun, DEDFs and 'ordinary' EDFs. Table 6.1 gives a list of numbering codes of each fibre along with the manufacturer. These numbering codes will be used in the following sections to refer to the individual fibres. Also listed are the individual linear birefringence, $\delta\beta_L$, the rotation coefficient, g, and the dispersion of the stress-optic coefficient, C (see Equation 5.47), obtained from a best fit simulation to each of the measured fibres. Note that C is related to g, through Equation 3.32, by a constant multiplier.

Fibre Number	Manufacturer	DGD (ps/km) at $\gamma = 0$	$\delta\beta_L$ (rad/m)	$\frac{\omega}{g}\frac{dg}{d\omega}$ with g = 0.14	Measured fibre lengths l (m)
S-SMF 1	Corning	0.21	0.26	0.089	114
S-SMF 2	Fibre Optics	0.24	0.29	0.092	114
S-SMF 3	Fibre Optics	0.29	0.35	–	56
DSF 1[1]	Corning	0.76	0.92	0.087	114 (76)
DSF 2[2]	Corning	1.55	1.88	0.090	114 (81)
DSF 3[2]	Corning	1.14	1.4	0.091	114
DSF 4[2]	Corning	2.1	2.55	0.089	114
DSF Spun 1	AT&T	< 0.05	–	0.105	114 (81)
DSF Spun 2	Lycom	< 0.05	–	0.108	114
DSF Spun 3[3]	Corning	< 0.05	–	0.092	114
DSF Spun 4[4]	Corning	< 0.13	–	–	114
DEDF 1	Corning	7.5	9.1	0.10	114
DEDF 2	BT Labs	14.4	17.5	–	113 (111)
EDF 1	BT Labs	364	442	–	3.6
EDF 2	BT Labs	6.3	7.7	–	2.8
EDF 3	BT Labs	17.6	21.4	–	3
EDF 4	BT Labs	8.3	10.1	–	3.2
EDF 5	BT Labs	59.2	72	–	3

Table 6.1 Numbering code of the measured fibre samples, along with the manufacturer and values, used to fit the measured data of DGD versus twist.

Some of the fibres, DSF 1, DSF 2 and DSF Spun 1, were measured in collaboration with BT Laboratories in Ipswich, England.

6.1.2.2 Measurement stability of the free-hanging fibre

[1] DS fibre from Corning with zero dispersion wavelength in the Er^{3+} window, see Appendix A.
[2] LS fibre from Corning with non-zero dispersion across the Er^{3+} window $\lambda_0 \geq 1.56\mu m$, see Appendix A
[3] From the same preform as DSF 3
[4] From the same preform as DSF 4

The measurement conditions of the free-hanging fibre in the tunnel were quite stable, the output SOP did not change with time (over a few hours), and the measured DGD could be usually repeated to within ±1 fs, both as a function of time and twist. One source of offset error for the absolute measured DGD were the short pigtails at the input and output of the fibre, which had a measured DGD value of about 3 fs. Repeatedly connecting and disconnecting the pigtails to the fibre under test, as had to be carried out when twisting the fibre at the front end, showed that the offset due to the pigtails introduced a standard deviation of ±1 fs from the mean measured DGD value. This error and also the small SOP rotation introduced by the fibre in contact with the bobbin at the far end of the catenary were neglected when comparing the analysis with the experimental results. In Section 6.4 the expected error in the measured absolute DGDs of the fibres will be estimated.

It is interesting that all the fibres showed twist rates up to 0.4 turns/m when unwound from their original shipping bobbins (taking care not to introduce twist). This twist is likely to arise during the fibre spooling process (due to shifting of the fibre bobbin) and would be impressed into the cabled fibre. The force acting along the fibre catenary measured, showed values of between 10 and 30 cN, which introduces a small DGD to the overall fibre DGD. This is caused by the short length at the fibre far end in contact with the bobbin, which is subjected to bending under tension.

6.1.2.3 Normalisation of the measured DGDs with respect to the measured fibre lengths

To compare the different fibre lengths the measured DGDs have been normalised with respect to the measured sample lengths in ps/km. This is consistent with Equation 5.45 which predicts a linear DGD increase with length for twisted fibres. But care has to be taken when translating this to fibre lengths larger than ~1 km where the local birefringence may change considerably along the fibre, and mode coupling becomes significant. It should be noted that the offset due to the pigtails included in the normalisation does not increase with fibre length. As the fibre lengths examined are short, less than 115 metre, the effect of change in birefringence, and also random mode coupling along the fibre, will be negligible on the measured DGD. (see Section 7.3). Thus the birefringence estimated from the DGD can be taken as the local fibre birefringence. In order that the reader can translate back to the measured differential group delay in *ps* in all the DGD versus twist plots, the lengths of the measured fibres will be shown, all of which were measured with better than a ±1 metre accuracy.

6.1.3 DGD reduction in elastically twisted fibres

6.1.3.1 DGD versus twist for S-SMFs

The measured values of DGD against twist for two S-SMFs from separate manufacturers are shown in Figure 6.2 (a) and (b). Both cases show a sharp decrease in DGD towards zero as twist is initially applied, followed by an increase at higher twist rates, and are in excellent agreement with the theoretical model given by Equation 5.45 which has been used to fit the measured data with the values given in Table 6.1.

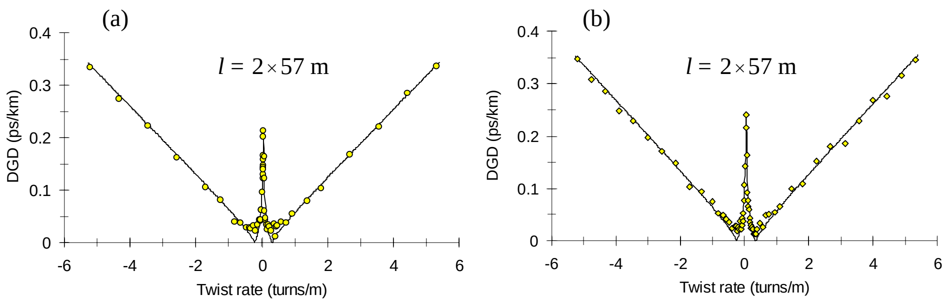

Figure 6.2 Measured and calculated values of DGD against twist for standard step-index fibres. In (a) for the S-SMF 1 and in (b) for the S-SMF 2.

The DGD for the applied twist[5] in Figure 6.2 (a) and (b) is as expected symmetrical about the zero twist position. The estimated linear birefringences is 0.26 rad/m and 0.29 rad/m for Figure 6.2 (a) and (b) respectively. Using these values in Equation 5.48 to estimate the twist rate needed to obtain zero DGD gives an ideal twist rate of around 0.28 turns/m for both fibres. Figure 6.2 shows that the measured DGD of the two fibres is a minimum when the twist is around 0.3 turns/m. The offset from zero is due to the pigtails. If the initial birefringence (DGD) is known, the ideal twist needed to null the DGD can therefore be calculated for each particular fibre. The measured DGD at zero twist for different lengths of S-SMFs is given in Table 6.1. The DGD values ranged from 0.2 to 0.3 ps/km (see also Figure 6.21). Comparing this measured DGD range with the simulated DGD due to core ellipticity in Figure 3.14, shows that the expected ellipticity in the measured S-SMFs is around 0.5%.

6.1.3.2 DGD versus twist for DSFs

[5] The fibre is twisted in opposite directions at the two fibre ends, so that the twist applied is effectively the same as for twisting at only one end of the fibre.

The measured values of DGD against twist for two dispersion shifted fibres, DSF 1 and DSF 2 are shown in Figure 6.3 (a) and (b) respectively. DSF 1 and 2 are both dispersion shifted fibres, DSF 1 is designed for zero dispersion λ_0 within the erbium window (1530 nm ≤ λ_0 ≤ 1560 nm), and DSF 2 for zero dispersion at λ_0 ≥ 1560 nm (Appendix A). Both fibres show a decrease in DGD towards zero followed by an increase at higher twist rates, similar to the S-SMF in Figure 6.2, again in excellent agreement with the theoretical model given in Equation 5.45, which has been used to fit the measured data [79] with the values given in Table 6.1.

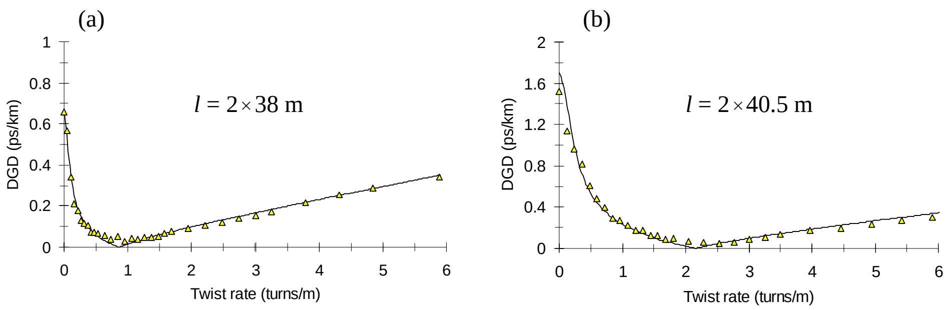

Figure 6.3 Measured and calculated values of DGD against twist for dispersion shifted fibres. In (a) for the DSF 1, and in (b) for DSF 2.

The DGD values at zero twist for the DSFs in Figure 6.3 are a factor of 5 to 10 times higher than the DGD values of the measured S-SMFs in Figure 6.2 (see also Figure 6.21). This agrees well with the simulation results in Section 3.3 which, assuming roughly the same ellipticity in the measured S-SMFs and DSFs ($e^2 \approx 0.5\%$), predicted a higher sensitivity to core ellipticity for DS fibre compared with S-SMF (by about a factor of 5). This is due to the higher index difference and smaller core diameter of the DSF. It should also be noticed that DSF 2 in Figure 6.3(b) show a higher DGD value at zero twist than DSF 1 in Figure 6.3(a), which may be due to the expected slightly higher index difference necessary to shift the zero dispersion wavelength of DSF 2 to a higher value, compared to DSF 1.

6.1.3.3 DGD versus twist for DS spun fibres

The measured DGD values against twist for the two commercially available dispersion shifted spun fibres DSF Spun 1 and the DSF Spun 2 are shown in Figure 6.4 (a) and (b) respectively. The spun fibres show in general a uniformly increasing DGD with increasing twist symmetrical about zero twist, as though they would have zero internal birefringence. These two spun fibres have an impressed sinusoidal spin [13], so it is not possible to untwist the fibre with uniform external twist, as it can be carried out for uniformly twisted spun fibre, to reveal the initial linear birefringence [169]. The data has been fitted simply by setting $\delta\beta_L$

= 0 in Equation (5.45) so that the DGD due to circular birefringence only is given by $\delta\tau = \delta\beta_C' \, l$ [84]. The values used for the dispersion of the stress optic coefficient are given in Table 6.1.

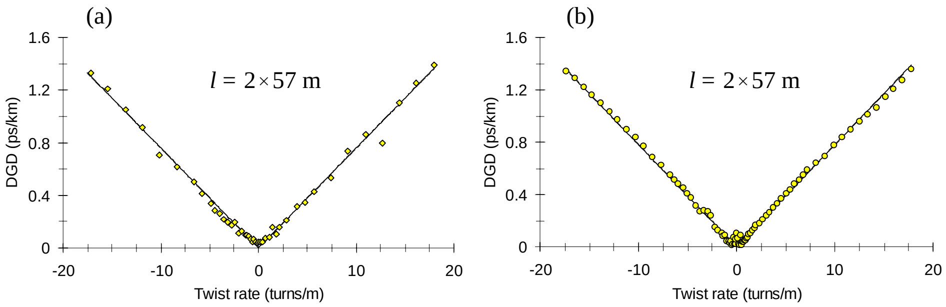

Figure 6.4 Measured and calculated values of DGD against twist for spun fibres. In (a) for the DSF Spun 1, and in (b) for the DSF Spun 2.

The measured DGD versus twist for the spun fibres shown in Figure 6.4 has been also plotted on an enlarged scale in Figure 6.5 showing more details about the measured DGD around the zero twist position. For the DSF Spun 1 in Figure 6.5(a) it can be seen that there is a very sharp small peak, of the same order as that in the measured S-SMFs. This peak is believed to be the remnants of the initial linear birefringence, indicating that the impressed spin in that fibre was not large enough to reduce the effective birefringence to virtually zero.

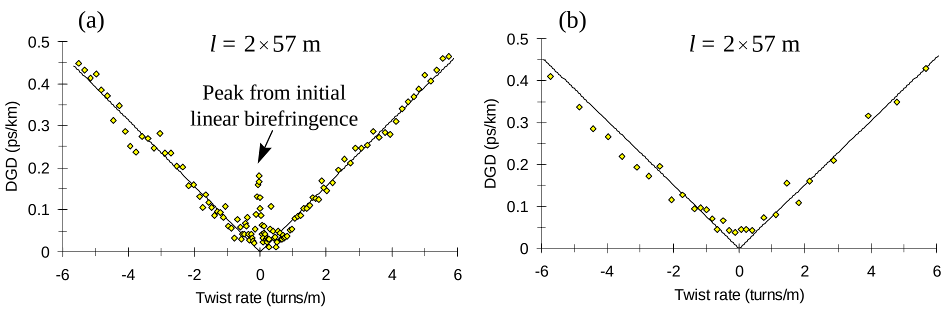

Figure 6.5 Measured and calculated values of DGD against twist for the spun fibres shown in Figure 6.4 but with enlarged scale. In (a) for the DSF Spun 1, and in (b) for the DSF Spun 2.

For the DSF Spun 2 in Figure 6.5(b) no such peak is visible, and the DGD at zero twist is close to zero. The offset, as mentioned before, is due to the fibre pigtails. In Section 6.3 spun fibres with different initial linear birefringence, and sinusoidal spin will be investigated in more detail.

6.1.3.4 DGD versus twist for DEDFs and EDFs

The PMD in EDFs can be an order of magnitude higher than for DSF [18], [117] which is mainly attributed to the smaller core diameter, higher refractive index difference and degenerated index profile from the wet phase aluminium doping which also causes large ellipticities of the fibre core (see Appendix C). For DEDF the PMD has been shown by us [117] to be an order of magnitude higher than DSFs, although DEDFs have the same refractive index profile and core diameter as the DSFs, as shown in Appendix C. In DEDFs no Al_2O_3 doping is used as in EDFs, and the erbium doping which is only about 20 to 70 ppb can be carried out using a vapour phase doping technique [86] (~2000 ppm in EDFs).

Measurement results for DEDFs: The DGD as a function of twist for one of the available DEDFs (DEDF 1) is shown in Figure 6.6(a). The high initial DGD of about 7.5 ps/km decreases towards zero, followed by an increase at higher twist rates. Again, the simulation results have been fitted to the measured data using Equation 5.45, with the values given in Table 6.1.

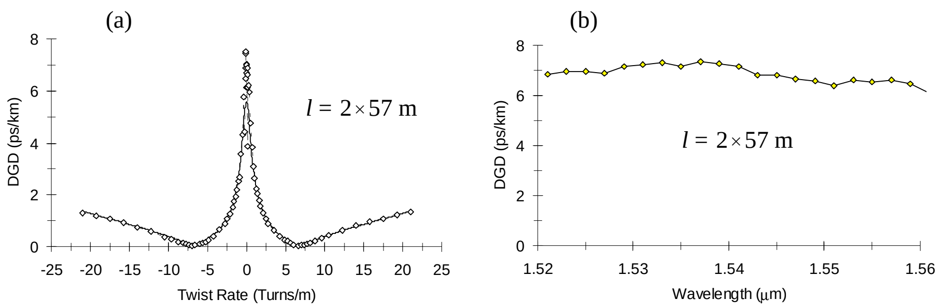

Figure 6.6 (a) Measured and calculated values of DGD against twist for the distributed erbium doped fibre DEDF 1, and in (b) the DGD versus wavelength close to zero twist.

The DGD at zero twist for DEDF 2 has been measured in the same way as for DEDF 1 shown in Figure 6.6(a) and the average DGD value measured at two different sections for DEDF 2 has been found to be 14.4 ps/km, as given in Table 6.1.

Next the profiles of the two DEDFs has been analysed in order to understand the origin of these high DGD values, which would be useful to know, in order to reduce the DGD in the next stage of DEDFs design. For DEDF 2 data about the core ellipticity measured on its preform using a preform analyser was available from BT Labs [86]. The measured ellipticity in the preform for DEDF 2 is around 7%, and it can be taken that this ellipticity was impressed into the fibre during drawing [86] (see also Appendix B for fibre manufacturing process). For this ellipticity the expected DGD for a DSF with step-index profile, considering shape and stress birefringence as discussed in Section 3.3 and shown in Figure 3.16, would be about 18 ps/km. This value is higher than that measured for DEDF 2, as would be expected following the discussion in Section 3.3, because the profile of DEDF 2 is not rectangular, and consequently the shape birefringence effect is not as sensitive to core ellipticity. Further, the cladding of DEDF 2 has been doped with P_2O_5 which reduces the thermal expansion mismatch between core and cladding and makes the fibre less sensitive to core ellipticity (see Appendix B).

For DEDF 1 no data from the preform was available, and the fibre has been scanned for core ellipticity by using a far field measurement of three fibre samples (carried out at NPL), and also by using electron microscope backscatter scans (Appendix C). For the measured DGD value of DEDF 2 a core ellipticity between 2 and 4 % would be expected, following from the results on DEDF 2 and the simulation results in Figure 3.1.6. However, from the far field measurement and also electron microscope scan, no core ellipticity was observable, as shown in Appendix C. For the far field measurement, this may be due to the fact that only three pairs of orthogonal scans were taken for the three different fibre samples Hence, there is a small chance of missing the core ellipticity in all three cases due to the 2% resolution of the far field measurement. The electron microscope on the other hand shows the whole fibre structure, but an important point to remember is that it cannot reveal core ellipticities below 5%. In order to understand the origin of the high intrinsic DGD value of DEDF 2, more precise measurement results would be necessary as e.g. by doing a complete two dimensional far field scan.

Figure 6.6(b) shows the measured DGD versus wavelength for DEDF 1, which shows nearly a flat trace over the measured wavelength range. The DGD versus wavelength plot could be also helpful, if performed over a larger wavelength (e.g. 1.3 to 1.6 μm), in understanding the intrinsic birefringence origin. From the theory in Section 3.3 we would expect a stronger wavelength dependence of the DGD due to shape birefringence, whereas for mainly stress birefringence, e.g. stress due to irregularities in the cladding frozen in during fibre manufacturing, we would expect a nearly flat trace.

The maximum anticipated PMD value for DEDFs used in ultra-high bit-rate long haul soliton systems which can be tolerated, has been calculated in Subsection 3.3.6, as ~ 0.1 $ps/\sqrt{km}$. Using a conservative 7 ps/km for the above DEDFs and using a ‘minimum’ expected coupling length of L_C = 100 m for the cabled fibre, as will be discussed in Section 6.4, the expected PMD may be calculated using Equation 3.36 as

$$PMD \approx \sqrt{L_C}\, DGD \qquad (6.1)$$

where the DGD is in units of ps/km, giving a resultant PMD for the above values of about $2\ ps/\sqrt{km}$, which is more than an order of magnitude higher than the maximum allowed value. This may be a problem if these DEDFs are used for ultra-high bit-rate, long haul soliton transmission systems [117]. The large intrinsic DGD may be reduced by spinning the fibre during drawing, which could be carried out by either applying uniform or sinusoidal spin, as will be discussed in Section 6.3. On the other hand, because the intrinsic DGD is so high, spinning, within the constraints of the fibre drawing process [13], may be not sufficient. It is therefore an important issue to reduce significantly the intrinsic origins of DGD, as e.g. core ellipticity in the next generation of DEDFs.

Measurement results for EDFs: The DGD as a function of twist for short lengths of EDFs (~3 m) was measured for four samples of different 'manufacturing ages', as listed in Table 6.1. EDF 1, which has the worst value, is one of the earliest made erbium doped fibres, whereas the other erbium doped fibres are more recent. The high values in the EDFs can be well understood by simply looking at the fibre profile as shown in Appendix C for some of the EDFs. The profile is severely degenerated due to the wet phase doping of the fibre with erbium and aluminium, and the core ellipticity has been measured at between 1 and 20% (see Appendix C) using the preform analyser and electron microscope backscatter scan.

In an erbium amplifier the EDF length is between about 10 and 30 metres and is usually coiled around a small spool. Spooling our measured EDFs around such a spool ($d \approx$ 15 cm), showed a reduction in the measured DGD of between 10 and 50%. In a link like TAT12, the EDFAs spacing is about 45 km [100], and over the distance of 6400 km there are about 140 amplifiers, whose overall PMD effect, including optical components like isolators[6], has to be minimised in order not to cause additional system limitations due to PMD. Realising the limitations of high PMD values, manufacturers seem to have addressed the problem by more careful manufacturing of their EDFs and choosing optical components, such as isolators, with

[6] Old isolators can show values of around 5 ps as we have measured, whereas nowadays polarisation insensitive isolators with PMD values < 0.05 ps and PDL < 0.1 dB are commercially available.

low PMD. The DGD in EDF, new or old, may be also reduced by applying elastic twist to the fibre with the appropriate twist rate as given in Equation 5.48.

6.1.4 DGD in fibres with left and right hand twist

By applying left and right hand twist to the two fibre halves with fixed centre point, as shown in Figure 6.7(a), the DGD versus twist has been measured for DSF 1 and DSF 2. The two lengths are from different sections of the same fibre bobbin as used for uniform twist in one direction, Figure 6.3. It can be seen in Figure 6.7(b) that now the DGD for the oppositely applied twist in the two fibre halves decreases towards zero without any increase in DGD at higher twists. This can be understood in the following way, the effective linear birefringence of the fibre reduces to zero in the same way as twisting the fibre in just one direction, and the polarisation dispersion caused by the circular birefringence is now cancelled because the light sees effectively left circular birefringence in the first half, and right circular birefringence in the second half, or vice versa, so that the group delay is ideally cancelled, assuming the same twist magnitude in both fibre halves.

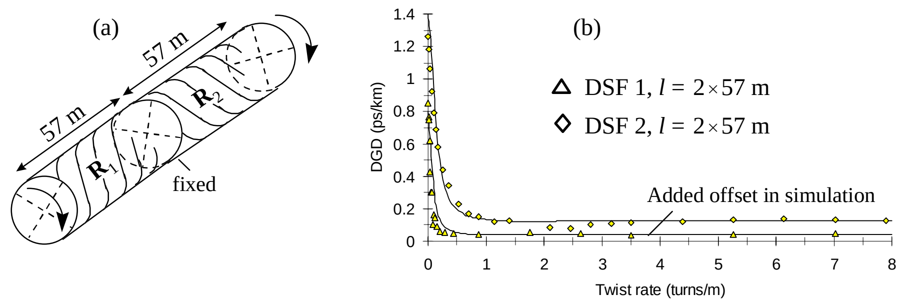

Figure 6.7 (a) Twisted fibre with opposite twist and fixed central point. In (b) measured and calculated values of DGD against twist for fibre twisted fibre with left and right hand twist.

The DGD matrix equation given in Equation 5.39, together with Equation 5.41, has been used to calculate the resultant DGD for the two fibre pieces with left and right hand twist, in order to fit the measured data in Figure 6.7(b). The simulation shows excellent agreement with the measured data. A small offset is added to the calculated DGD values to improve the fit between the measurement and simulation. The offsets in the measured data in Figure 6.7(b) are due to the pigtails, and due to the difficulty in applying twist of exactly equal amounts, but opposite sign, to the two fibre halves. This highlights one of the main difficulties (sensitivity) of the above method of reducing the DGD. The same effect of generating left and right hand twist in the fibre could also be obtained by twisting the fibre just at the centre point and keeping the fibre ends fixed, which would ensure equal amount of twist in the two fibre halves, assuming equal lengths. Small amounts of twist introduced into the fibre have been used to reduce the PMD in cabled fibres [12].

The above idea of twisting a fibre with opposite twist direction is interesting because the fibre DGD now ‘ideally’ continuously decreases to zero for increasing twist, similar to spun fibre. This idea is not new and has been considered theoretically before in a similar form in Reference [37], to interchange the fast-slow mode of the fibre. The drawback with the above method is the need to exactly balance the oppositely applied twists to get equal magnitudes of circular birefringence with opposite sign in the two fibre halves, and also to keep the twisted fibre in position.

6.1.5 DGD as a function of external stress in different fibres

In this subsection the effect of external pressure on different fibres (with different profiles) without and with external applied twist on the DGD has been investigated. Cabling on one hand provides a protective package, a buffer for the optical fibre from mechanical stresses presented by the environment. On the other hand, if it is not properly designed it can induce a stress on the fibre during manufacture [12]. In cables using the tight buffered design, lateral loads on the fibre of a few grammes/mm may be experienced [100]. This can induce a higher net birefringence leading to a higher PMD, rather than acting as a source of random mode coupling to reduce the PMD along the cabled fibre (see also Subsection 6.4.2). This is especially true when using spun fibre, which has close to zero uncabled DGD as shown in Subsection 6.1.3.3. For that reason it is interesting to know if a fibre with elastic twist would be more resistant to PMD induced by cabling.

By applying external pressure to a fibre as shown in Figure 6.8, by squeezing the fibre between two parallel plates, stress birefringence $\delta\beta_S$ is introduced as given in Equation 3.31. For a uniformly twisted fibre, assuming no internal linear birefringence, with uniform external applied pressure, the resultant birefringence vectors are fixed and orthogonal to each other on the Poincaré sphere. The resultant birefringence for a twisted fibre with external pressure is $\delta\beta = \sqrt{\delta\beta_S^2 + \delta\beta_C^2}$ and the frequency derivative determining the dispersion is given by

$$DGD = \left(\frac{\delta\beta_S \delta\beta_S' + \delta\beta_C \delta\beta_C'}{\sqrt{\delta\beta_S^2 + \delta\beta_C^2}} \right) \tag{6.2}$$

where, for the dispersion of the stress birefringence we also consider now the dispersion of the stress-optic coefficient so that

$$\delta\beta_S' = \frac{\delta\beta_S}{\omega} \left(1 + \frac{\omega dC}{C d\omega} \right) \tag{6.3}$$

In Figure 6.9(a) the DGD versus external applied pressure has been calculated for a fibre length of 1.5 metre at different twist rates. The outer fibre radius has been taken as 125/2 μm in the calculation. The slope of the DGD versus external pressure for zero twist has been calculated as 0.23 ps/(km•N). For twisted fibre, up to 8 turns/m, the calculated DGD versus external pressure showed hardly any difference in the slope to that at zero twist. Increasing the twist rate above 8 turns/m the circular birefringent fibre starts to show reduced sensitivity to the external pressure, but at the cost of a growing offset DGD at zero external pressure.

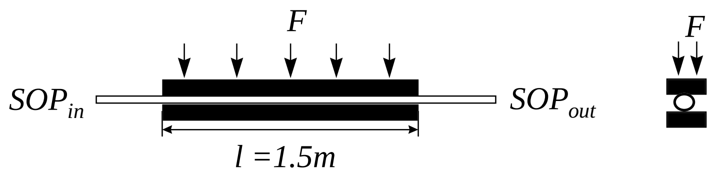

Figure 6.8 Experimental set-up to applying uniaxial pressure to the fibre. The input and output of the fibre are connected to the PMD measurement equipment.

Figure 6.9(b) shows the DGD versus external pressure at different twist rates for 1.5 m of fibre, DSF Spun 2, for which we can assume that the effective internal birefringence is close to zero. The slope of the measured DGD versus stress, using a linear first order best fit, showed a nearly constant value around 0.13 ps/(km•N) for twist rates of 0 to 8 turns/m within the measurement accuracy for the measured short length of fibre, as predicted by simulation result. However, comparing the measured slope with the predicted slope from the simulation shows a difference by about a factor of two. This factor of ~2 difference originates most probably from the fact that the calculated results assume a uniform applied force along the fibre, whereas in the measurements there will always be some small irregularity in the pressure along the fibre. Another factor which affects the slope of the DGD versus pressure is the fibre coating as shown in [12], which for a larger diameter coating distributes the acting pressure more widely so that the applied force does not act as a sharp line force along the fibre, and the sensitivity to external pressure is reduced.

An interesting result we could also observe was the relaxation time of the fibre to adapt to the external applied pressure. It took up to about 15 minutes for the fibre to settle down (for a force of about ~ 25 N/m), and before repeatable measurement results within ±0.2 fs could be taken. Measuring the DGD versus pressure with 16 and 32 turns/m external applied twist did not show any noticeable difference in the measured slopes shown in Figure 6.9(b), which is most probably due to the measurement accuracy and the large offset at zero pressure for these high twist rates.

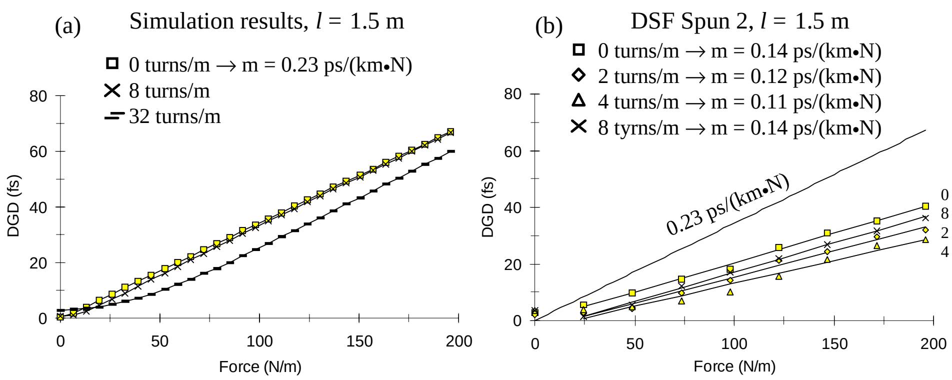

Figure 6.9 DGD against external applied pressure at different twist rates in (a) calculated, and in (b) measured for DSF Spun 2.

From above we can conclude that elastic twist as a means to reduce the fibre sensitivity to external pressure shows no effectiveness for sensible twist rates up to 8 turns/m. Reduction of stress, for the embedded fibres, by using a modified cable design (see Subsection 6.4.2.2), in order not to introduce additional PMD into low DGD fibres, e.g. spun fibres, seems to be the more appealing solution for cable manufacturer [12]. The difference in the slope has been also observed by measuring the DGD versus external pressure for S-SMFs and DSFs. The measured fibres (S-SMF, DSF and spun DSF), have nearly the same outer diameter coating (fibre jacket) of ~ 240 μm ± 10 μm, which may explain why the measured fibres showed the same slope.

6.2 DGD in forward-backward direction as a function of twist

The experimental set-up for measuring the DGD of the light reflected from the far end face of a cleaved fibre (Fresnel reflection) as a function of twist [170], [171], is shown in Figure 6.10 (see also Appendix D for picture). This experiment not only helps in determining the zero twist position experimentally but also shows whether fibre with reflection behaves reciprocally, which will be important for analysing the measured POTDR traces in Chapter 7. If the fibre behaves reciprocally we would expect the DGD of the fibre at the zero twist position for the forward and backward path to be twice that compared to a single way measurement. Moreover, because the reflected light (for the path reversal) sees an opposite handedness of twist to that in the forward direction, the twist induced dispersion is cancelled (see Subsection 6.1.4).

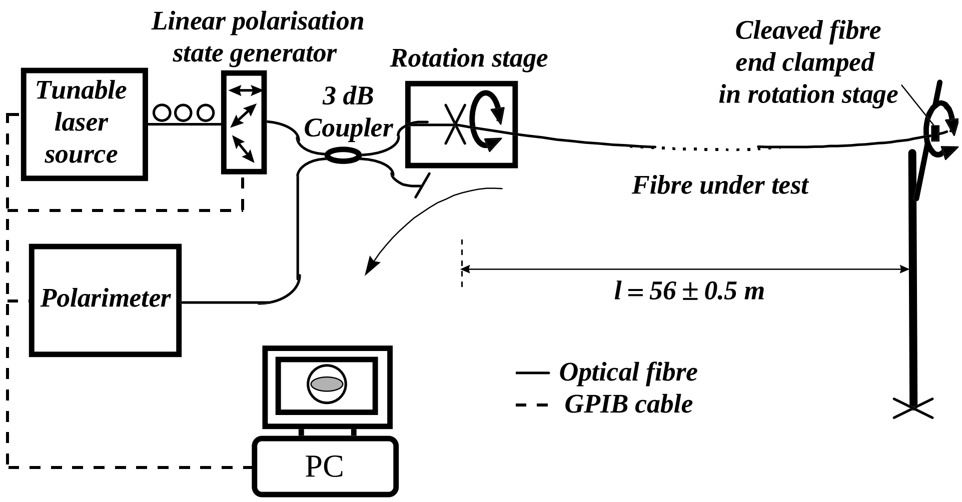

Figure 6.10 Set-up for measuring DGD of twisted fibre with reflection at the far end. See also Appendix D for picture of twisting fibre at far end.

For a well-cleaved fibre the reflected power is about 14 dB below the incident power (due to Fresnel reflection for a glass to air interface, Section 2.5). This power loss does not include the 2×3 dB loss induced from the 3 dB coupler for the forward-backward direction. The DOP of the reflected light was fully polarised (100%), as was the incident light. In Figure 6.11(a) and (b), the DGD as a function of twist for S-SMF 3 and in DSF 1 are shown respectively, which, as expected for both fibres, tends towards zero DGD for increasing twist neglecting the offset. The offset for the backscatter measurement was slightly higher than in forward direction only, due to the 3 dB coupler, and was about 5 fs which gives the offset of 0.09 ps/km for the 56 m as shown in Figure 6.11.

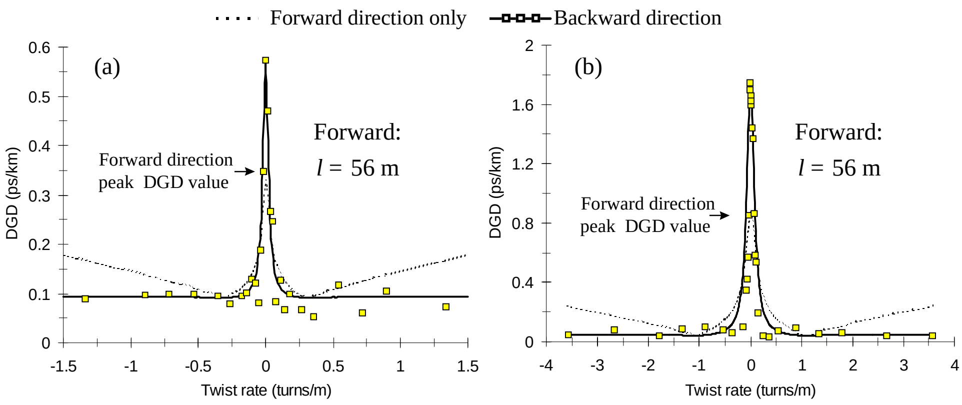

Figure 6.11 Measured and calculated values of DGD against twist for light reflected from far end of the fibre. In (a) S-SMF 3 and in (b) DSF 1

The measured DGD at zero twist for the S-SMF 3, as shown in Figure 6.11(a), is 32 fs for the 56 metre fibre in forward-backward direction. This value is twice that for a single way measurement and implies that the fibre has a DGD of 16 fs over 56 m (0.29 ps/km). Comparing this value with the one measured at zero twist for S-SMF 2 in Figure 6.2(b), which is from the same manufacturer, shows that this is indeed the value expected in just forward direction within the error due to the pigtails. The same is true for DSF 1 where the DGD at zero twist for the forward-backward direction in Figure 6.11(b) is ~ 1.75 ps/km and for the same fibre, the DGD in Figure 6.3(a) and Figure 6.7(b) has been measured as ~ 0.7 and 0.9 ps/km respectively.

Of more interest than the absolute DGD at zero twist is that the DGD for the twist rates shown in Figure 6.11 (a) and (b) reduces towards zero for increasing twist, as expected from the theory, due to the cancellation of the twist induced dispersion in the forward-backward direction. The DGD of the measured data in Figure 6.11 (a) and (b) has been fitted using the DGD matrix equation given in Equation 5.39, together with Equation 5.41, where the resultant fibre matrix is given by a rotation-reflection-rotation matrix. The backward rotation matrix is given by the transpose of the forward matrix, or equivalently, it can be described by a reflection-rotation matrix [170] (Section 7.2). In describing the fibre by a reflection-rotation matrix the rotation can be shown to be composed of two equal matrices but with left and right hand twist [170] (Section 7.2), which is the same as for the fibre in Section 6.1.4. As the reflection, defined in Equation 2.21, is assumed to be wavelength independent it can be understood that the DGD for both the fibre with left and right hand twist and the twisted fibre with backreflection is basically the same function with twist. Figure 6.11 also shows the DGD versus twist as expected in the forward direction only for the corresponding fibres.

An interesting effect has been observed by measuring the DGD versus twist of the backreflected light for the two fibres, S-SMF 3 and DSF 1, with very large twist rates as shown in Figure 6.12. The DGD from theory should go towards zero for increasing twist as discussed above, but as can be seen in Figure 6.12, the DGD above twist rates of 2 and 5 turns/m for S-SMF 3 and DSF 1 increases, and resembles a step function.

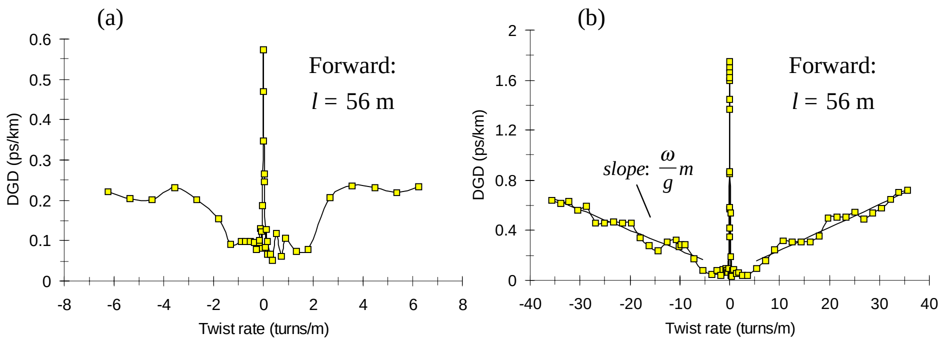

Figure 6.12 Measured and calculated values of DGD against twist for light reflected from far end of the fibre. In (a) for S-SMF 3 and in (b) for DSF 1.

The slope of this step function, as indicated in Figure 6.12(b) for DSF 1, has been calculated using a least square fit to be $m \bullet \omega / g = 0.012$, where the slope has been normalised to ω and $g = 0.14$, and accounting for the factor of two of the go and return path. Comparing this value with the measured values for the normalised dispersion of C as given in Table 6.1 shows that this value is just ~1/7 of the dispersion value for the stress-optic coefficient. The origin of this ‘higher order’ twist effect, is at the moment not understood, but this effect may be associated with some weak stress-related linear birefringence induced in the fibre. Moreover, it could be suggested by comparing Figure 6.12 (a) and (b), that this effect may be related to the magnitude of the linear birefringence. For the higher linear birefringence fibre in Figure 6.12 (b), which also has a different fibre profile, the ‘unexpected’ twist effect starts at a higher twist rate than for the lower birefringence fibre in (a). More measurements of different fibres would be necessary to better understand the origin of this twist effect. This effect has not been reported as far as we know, and although it may be interesting from the physical point of view it is nevertheless quite small and may be neglected, because we would not expect more than 1 turn/m of elastic twist in an optical fibre, or cabled fibre, if not twisted on purpose (see Subsection 6.1.2.2).

6.3 DGD in spun fibres with different initial linear birefringence as a function of externally applied twist

In Section 5.4, the spun fibre with sinusoidal spin determined by the two parameters, spin amplitude and spin period, of the alternating spinning process, have been introduced together with the numerical simulation to calculate the DGD reduction in this type of fibre. This section a detailed analysis of how the joint interactive effect of these two parameters with the initial linear birefringence determines:

(a) the intrinsic overall DGD of the resultant fibre when no external twist is applied to it;
(b) how this zero twist DGD value changes when the fibre is subjected to external twist.

It will be seen that if the sinusoidal spin in these spun fibres is not high enough (relative to the initial linear birefringence), this can lead to high peak DGD values at, and close to zero external applied twist [172]. At the end of this section an approximate equation will be given for the necessary effective sinusoidal spin, $\tilde{\gamma}_{rms}$, to reduce the 'starting' fibre DGD (at zero external twist) close to zero for fibres with different initial linear birefringence values.

The idea of using external twist to analyse spun fibre was demonstrated in [106] for spun fibre with uniform spin, in which case the fibre was simply 'unspun' to zero spin revealing the initial linear birefringence and the spin rate of the fibre. For the fibre with sinusoidal spin this is not so simple, because the spin period of this fibre is < 2 metre and the spin rate larger than 4 turns/m [13].

6.3.1 DGD as a function of external applied twist for DS fibres and Spun fibres from the same preform

The DGD as a function of externally applied twist has been measured for two dispersion shifted fibres DSF 3 and DSF 4, and two dispersion shifted spun fibres DSF Spun 3 and DSF Spun 4. These fibres DSF 3 and DSF Spun 3 were made from the same preform, and DSF 4 and DSF Spun 4 from another, as indicated in Table 6.1. The four fibres have been manufactured for research purposes and no information was released about the spin rates used in these fibres.

First, the DGD of the two dispersion shifted fibres was measured in order to estimate the initial linear birefringence. The measured values of DGD against twist for two dispersion shifted fibres, DSF 3 and DSF 4 are shown in Figure 6.13 (a) and (b) respectively. Both dispersion shifted fibres are non-zero dispersion shifted fibres similar to DSF 2 (Figure 6.3(b)). Both DSFs in Figure 6.13 show as expected a decrease in DGD towards zero followed by an increase at higher twist rates, in agreement with the theoretical model given in Equation (5.45), which has been used to fit the measured data with the values given in Table 6.1.

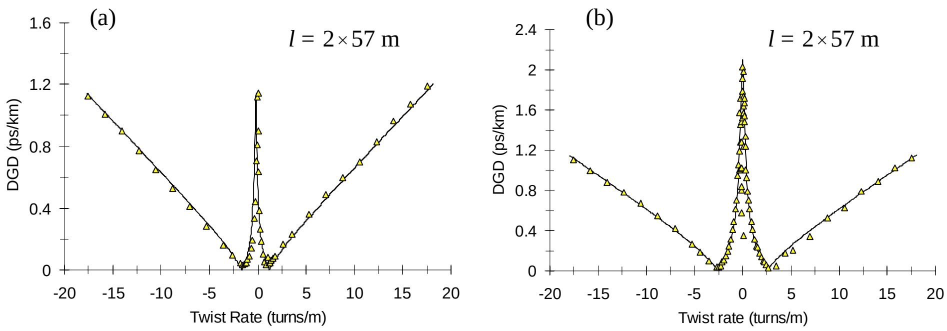

Figure 6.13 Measured and calculated values of DGD against twist. In (a) for DSF 3 and in (b) and DSF 4.

DSF 3 and DSF 4 have a difference in their DGD at zero twist by about a factor of two, indicating that the linear birefringence of the two fibres also differs by a factor of two. This difference in linear birefringence has a significant influence on the performance of the spun fibre made from these two preforms, as we will see next.

The measured values of DGD against twist for the two dispersion shifted spun fibres, DSF Spun 3 and DSF Spun 4 are shown in Figure 6.14 and Figure 6.15 respectively. In Figure 6.14 (a) and (b), one can see that DSF Spun 3, which has the same parent preform as DSF 3, has a virtually zero DGD at zero twist and its DGD grows nearly linearly with twist, as we would expect for such a spun fibre with sufficient spin (compared with DSF Spun 1 and DSF Spun 2 in Figure 6.4). Equation 5.45 with $\delta\beta_L = 0$ has been used to fit the measured data in Figure 6.14 with the value used for the dispersion of C given in Table 6.1. We can say that for the spun fibres DSF Spun 1, 2 and 3, the effective birefringence (not locally) has been virtually zeroed, so that the DGD measured in these fibres is also close to zero.

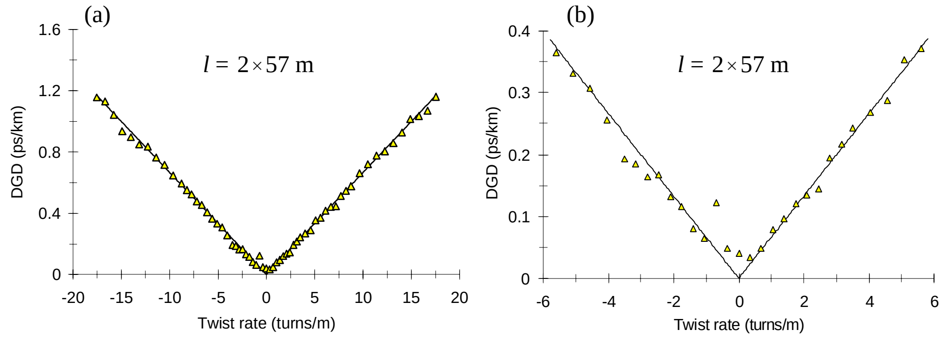

Figure 6.14 Measured and calculated values of DGD against twist for DSF Spun 3. In (a) over a large twist range and in (b) over a small twist range.

However, DSF Spun 4 in Figure 6.15, which has the same parent preform as DSF 4, behaves very differently from DSF Spun 3, in that the DGD around zero twist fluctuates significantly with twist, and the peaks are up to half the DGD value of DSF 4 at zero twist. From the system application point of view, this type of DGD fluctuation versus twist is highly undesirable, because in the process of fibre manufacturing, cabling and cable laying, some twisting is often unavoidable.

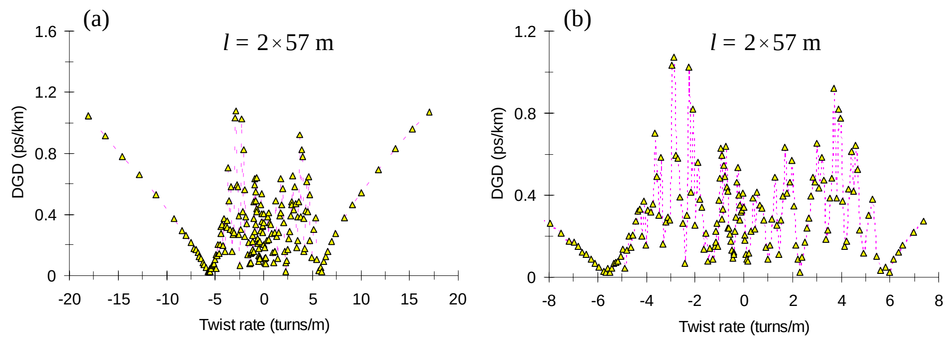

Figure 6.15 Measured DGD values against twist for DSF Spun 4. In (a) over a large twist range and in (b) over a small twist range.

6.3.2 Simulation of the DGD of Spun fibre with different initial linear birefringence and spin as a function of external twist

In order to understand the different behaviours of DSF Spun 3 and 4, numerical simulations were carried out. The initial linear birefringence of DSF Spun 3 and 4 has been estimated from DSF 3 and DSF 4, which have the same parent preform respectively, by using Equation (5.46) at λ = 1.55 μm to be $\delta\beta_L$ = 1.4 and 2.55 rad/m respectively. This was then fed into the simulation program as the initial linear birefringence values ($\delta\beta_L$) for DSF Spun 3 and 4, and the DGD versus external twist was simulated with different spin amplitudes A_γ, and periods

Λ_γ, assuming that the fibre has a sinusoidal spin style. The input SOP and $\Delta\lambda$ around the centre wavelength at 1.55 μm, have been chosen to achieve minimum error in the calculated DGD as discussed in Section 5.4. The simulated fibre length has been chosen between 16 and 30 metres in order to keep the simulation time reasonable, but also to allow a few periods of the sinusoidal spin within the total fibre length. The measurement and simulation results of the spun fibre with sinusoidal spin have been normalised to (ps/km), as carried out for all the results before, although a fluctuation has been observed in the measurement and simulation of the DGD versus external twist in some of the spun fibres. This fluctuation grows linearly with length as shown in Appendix B for simulated fibre lengths from 16 to 200 metres confirming the validity of the step to normalise the calculated DGD values.

6.3.2.1 Simulation results for $\delta\beta_L$ = 2.55 rad/m as expected for DSF Spun 4

At first, in order to show the good agreement between the numerical simulation and the analytical solution derived for uniformly twisted fibre, the estimated linear birefringence of the DSF 4 ($\delta\beta_L$ = 2.55 rad/m) has been fed into the program to calculate the fibre DGD, as a function of external applied twist with no internal spin. Comparing the numerical simulation result (circles in Figure 6.16(a)) with the analytical calculated values from Equation 5.45 (solid line in Figure 6.16(a)), shows that the results are virtually identical.

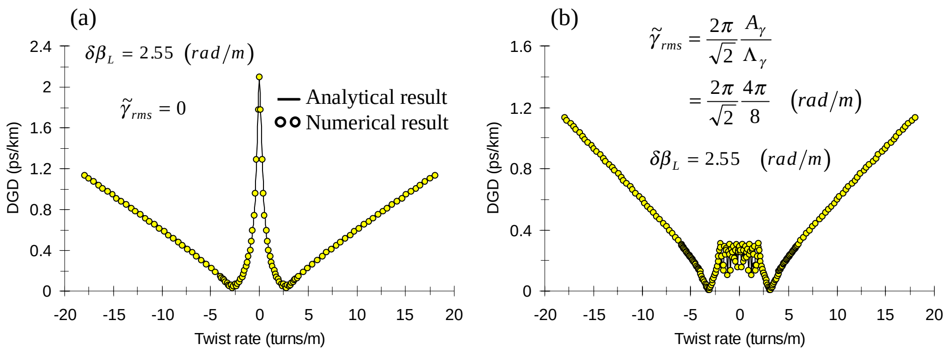

Figure 6.16 Numerical calculation of DGD versus external applied twist. In (a) for the unspun fibre DSF 4 and in (b) for DSF Spun 4 with $\tilde{\gamma}_{rms} \approx$ 1.1 turns/m.

Next, in Figure 6.16(b) the dispersion shifted fibre, DSF 4, has been simulated with internal spin for the calculation of the DGD versus twist of DSF Spun 4. The amplitude of the internal spin has been chosen as $A_\gamma = 4\pi$ radians and the spin period Λ_γ = 8 m. It can be seen in Figure 6.16(b) that the effective spin $\tilde{\gamma}_{rms} \approx$ 1.1 turns/m (Equation 5.54), is not large enough to zero the starting DGD at, and around zero external twist. The DGD in Figure 6.16 (b) at zero external twist is about 15% of that in Figure 6.16(a) at zero twist. In Figure 6.17 the DGD versus external twist has been calculated for DSF Spun 4 ($\delta\beta_L$ = 2.55 rad/m) as in Figure 6.16(b) but now with a quarter of the spin period as used above, so that $\tilde{\gamma}_{rms}$ ≈ 4.4 turns/m.

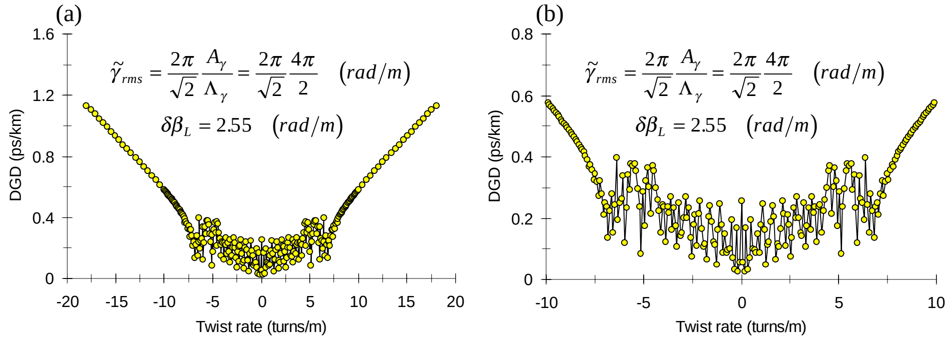

Figure 6.17 Numerical calculation of DGD versus external applied twist for DSF Spun 4 with $\tilde{\gamma}_{rms}$ ≈ 4.4 turns/m. In (a) over a large twist range and in (b) over a small twist range.

Comparing Figure 6.17(a) with Figure 6.16(b) shows that the fluctuation of the DGD with external twist has broadened to higher external twist rates before the dispersion due to the external twist becomes dominant, whereas the peaks in the DGD versus twist stay roughly at the same magnitude. Figure 6.17 for the chosen effective spin shows an interesting similarity to the measured DSF Spun 4 case in Figure 6.15, in the way the DGD evolves with external twist. However, the peak to peak value of the DGD fluctuation versus twist in Figure 6.15 is far higher than the one predicted by the simulation in Figure 6.17. This could be due to the fact that in the measured fibre (Figure 6.15), the twist in the two fibre sections have slightly different magnitudes. The simulation results of such spun fibres with different fibre lengths (see Appendix B for fibre lengths l from 16 to 200 metres metre), showed that this fluctuation grows linearly with length, justifying the normalisation in (ps/km) used in the Figures.

For the higher effective spin values of 8.9 and 17.8 turns/m, as shown in Figure 6.18 (a) and (b), the DSF Spun 4 starts now to behave, in its DGD versus external twist, as we would expect for such a spun fibre with overall DGD close to zero at zero twist, indicating that the effective spin in this fibre is now large enough.

In Appendix B (Figure B.5(a)) the DGD versus external twist has been also plotted for an effective spin rate of $\tilde{\gamma}_{rms}$ = 8.9 turns/m as used in Figure 6.18(a), but by using double the spin amplitude A_γ, and half the spin periods Λ_γ, which showed (as expected), roughly the same effective DGD reduction in DSF Spun 4, because the same effective spin has been used. On the other hand, doing a range of simulations with different A_γ and Λ_γ but maintaining $\tilde{\gamma}_{rms}$ constant showed that the spin amplitude A_γ should be chosen above 2π radians in order to ensure at least one complete rotation of the internal fibre axes. Moreover, it was possible to see that doubling the twist amplitude A_γ, rather than choosing half the spin period, showed a slightly stronger effect on the DGD reduction in spun fibre.

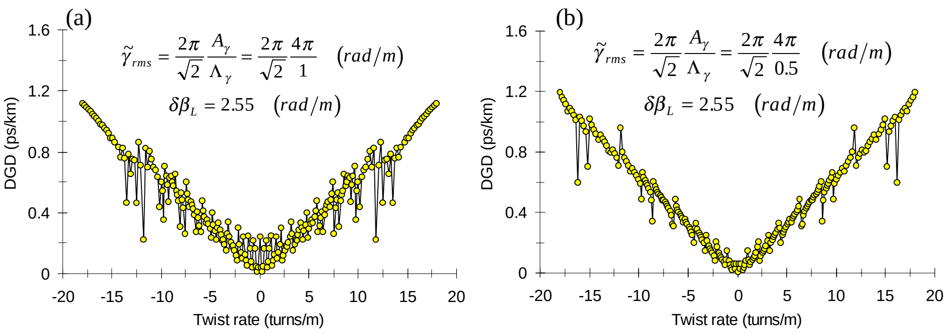

Figure 6.18 Numerical calculation of DGD versus external applied twist for DSF Spun 4. In (a) for $\tilde{\gamma}_{rms} \approx 8.9$ turns/m and in (b) for $\tilde{\gamma}_{rms} \approx 17.8$ turns/m.

6.3.2.2 Simulation results for $\delta\beta_L$ = 1.4 rad/m as expected for DSF Spun 3

In Figure 6.19(a) and (b), the simulation results are shown for DSF Spun 3 with $\delta\beta_L$ = 1.4 rad/m and using effective spins of 1.1 and 4.4 turns/m as used for DSF Spun 4 in Figure 6.16(b) and Figure 6.17 respectively.

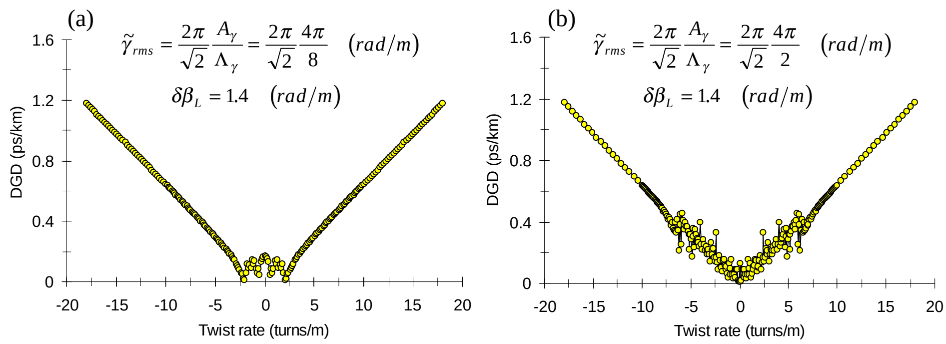

Figure 6.19 Numerical calculation of DGD versus external applied twist for DSF Spun 3. In (a) for $\tilde{\gamma}_{rms} \approx 1.1$ turns/m and in (b) for $\tilde{\gamma}_{rms} \approx 4.4$ turns/m.

It can be seen in Figure 6.19(a) that the effective spin of 1.1 turns/m seems to be too low to obtain a zero overall DGD at and around zero external twist. However for $\tilde{\gamma}_{rms}$ = 4.4 turns/m, Figure 6.19(b), DSF Spun 3 shows, even at this 'low' spin rate (compared with DSF Spun 4), a DGD versus external twist behaviour which is approaching the measured value on DSF Spun 3, as shown in Figure 6.14, and represents a well-behaved spun fibre.

It is interesting to notice that for $\tilde{\gamma}_{rms}$ = 4.4 turns/m, the simulated DGD versus external twist for both DSF Spun 3 and DSF Spun 4, in Figure 6.17 and Figure 6.19(b), show close similarity to those measured in Figure 6.14 and Figure 6.15 respectively. For the effective spin values of 8.9 and 17.8 turns/m, as shown in Figure 6.20 (a) and (b) respectively, the DSF Spun 3 shows now nearly no local fluctuations anymore in its DGD with external twist, again highlighting the good behaviour of the spun fibre with sufficiently large values of spin.

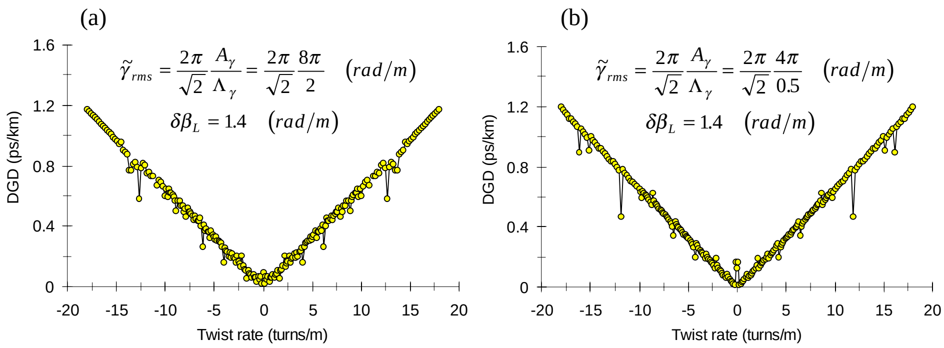

Figure 6.20 Numerical calculation of DGD versus external applied twist for fibre with sinusoidal spin and initial linear birefringence as estimated for DSF Spun 3. In (a) for $\tilde{\gamma}_{rms} \approx$ 8.9 turns/m and in (b) for $\tilde{\gamma}_{rms} \approx$ 17.8 turns/m.

6.3.3 Review of the results for the spun fibre with sinusoidal spin in comparison to spun fibre with uniform spin.

6.3.3.1 Minimum sinusoidal spin for manufacturing fibres with low DGD

Noting the good agreement between the experimental and simulation results, the following conclusions of spun fibre with sinusoidal spin can be made. When subjected to an external twist, spun fibre with a sinusoidal spin should show, if the spin rate is high enough, a uniform increase in DGD as if the fibre did not possess any internal linear birefringence. Moreover, by performing a range of simulations (see also Appendix B), an empirical value for the minimum effective spin needed, in order to achieve sufficient DGD reduction in such fibres, has been obtained in terms of the fibre intrinsic linear birefringence as

$$\tilde{\gamma}_{rms} > 4 \cdot \delta\beta_L \qquad (turns/m) \tag{6.4}$$

If the spin (as specified in Equation (6.4)), is not high enough so that the starting DGD is not reduced sufficiently, peaks up to half the height of the starting DGD can occur, which could result in a higher PMD in an overall link.

6.3.3.2 Review on necessary elastic twist or uniform spin to produce low DGD fibres

In summary, the different twist methods (elastic twist or spin as used in this chapter) may be compared in their efficiency in reducing the DGD in fibres with the same initial linear birefringence, as for example for the fibres listed in Table 6.1. The necessary twist rate to get sufficient DGD reduction may be estimated using the following equations. For DGD reduction using uniform external twist the ideal twist rate as given in Equation (5.48) can be written as

$$\gamma \approx \pm\delta\beta_L \quad (turns/m) \tag{6.5}$$

It should be noted again that the external applied uniform twist has the disadvantage that the DGD is at a minimum only at that twist rate. For spun fibre with uniform spin, and also for fibre with external alternating left and right hand twist, the minimum spin or external twist necessary to get at least a 95% DGD reduction from the starting DGD can be found from Equation (5.49) as

$$\gamma > 2 \cdot \delta\beta_L \quad (turns/m) \tag{6.6}$$

For spun fibre with sinusoidal spin the minimum spin is specified in Equation (6.4) as a function of the initial linear birefringence, and its efficiency in the DGD reduction (at zero external twist) for $\delta\beta_L$ < 4 rad/m is about of the same order as the one specified for spun fibres with uniform spin given in Equation (6.6).

6.3.3.3 Comparison of the DGD reduction in spun fibre with uniform and sinusoidal spin from a manufacturer's point of view

From Equation (6.6), we may calculate the necessary uniform spin to minimize the DGD of a fibre which exhibits, say, a linear birefringence of $\delta\beta_L$ = 3 rad/m, covering the birefringence values measured for S-SMFs and DSFs as listed in Table 6.1, as being γ > 6 turns/m. In fibre manufacturing, a typical drawing speed is about 10 m/second [13] from which the necessary rotational speed for example of the preform may be estimated to be 3600 rotation per minute. This necessary rotation speed may be above the maximum practical rotation speed in commercial fibre production [13], although in Reference [110], spun fibre has been drawn with uniform rotation rates of the preform up to 2000 rotations per minute (RPM).

If spinning the above fibre with a sinusoidal spin, in order to reduce the DGD, the effective spin rate $\tilde{\gamma}_{rms}$, as given in Equation (6.4), should be larger than 12 turns/m. If choosing a spin period Λ_γ of 2 metre [13], then the sinusoidal spin amplitude should be larger than 34 radians (see Equation 5.54). It seems possible to achieve these kind of parameters in commercial fibre production as has been shown in [13], where effective spin rates larger than 12 turns/m have been used.

From the point of commercial fibre production, sinusoidally spun fibre seems to have an advantage over uniformly spun fibre, although the effective spin necessary for the sinusoidal spin technique seems to be higher than the comparable uniform spin. Further work is still needed in order to understand whether the sinusoidally spun fibre shows an advantage in the presence of random perturbations, because the rotational frequencies are changing periodically along the fibre as suggested in [13]. This could be carried out by extending the numerical simulation model to include some random birefringence and mode coupling along the fibre. More simulation would also be necessary to understand more fully the large fluctuation terms (and perhaps also their temperature dependence) observed in spun fibre when the effective spin is not high enough. It may also be interesting to investigate the DGD reduction in spun fibre containing more than one rotational frequency.

6.4 Collation of the measured short length DGD values with expected polarisation mode coupling lengths in long lengths of fibres

In this section, the expected errors in the DGD values in Table 6.1 will be estimated. The PMD on the shipping bobbin has been measured (fibre lengths > 2 km) for some of the fibres from which the intrinsic DGD has been investigated. This allowed calculation of the expected mode coupling length of spooled fibres. More importantly, the expected range of polarisation mode coupling lengths for cabled fibres needs to be estimated, in order to estimate the PMD in fibres under field conditions, which could be obtained from external sources about the cabling effect on fibre PMD.

6.4.1.1 Review of the measured data

In Table 6.1 the measured fibres along with the manufacturer, are listed together with the values used in the simulation to fit the experimental data of the DGD versus twist. The values used to obtain the best fit, at the centre wavelength λ = 1.55 μm, are the DGD at zero twist, the linear birefringence $\delta\beta_L$ which is estimated using Equation 5.46 as $\delta\beta_L$ = DGD•ω, and the normalised wavelength dependence of the stress-optic coefficient given by $\omega/g{\bullet}dg/d\omega$, where g has been taken as 0.14. For the EDFs, only a few metres of fibre were measured versus twist and the DGD and $\delta\beta_L$ are the directly measured and estimated values at zero twist respectively. For EDFs, the loss without pumping is quite high (~ 2 - 6 dB/m at 1.53 μm) depending on doping level), which only allowed measurement of short lengths of fibres. On the other hand this was sufficient for the required DGD resolution because of the large intrinsic DGD encountered in the measured EDFs. In Table 6.1 the given DGD values are often the average value measured from different sections of the same fibre.

6.4.1.2 Expected error in the measured values in Table 6.1

The error in the measured absolute DGD values, at zero twist, given in Table 6.1 can be estimated in the following way. At first, the corresponding DGD value in ps for the actual measured fibre length has to be calculated from the given normalised DGD value by multiplying by the given fibre lengths. For these DGD values the error can be assumed to be < 10 fs, which includes the error due to the offset from the pigtails, the error in the measured fibre length and the measurement accuracy of the PMD equipment itself. The expected error in the absolute DGD at zero twist for the measured S-SMFs and DSFs, given in Table 6.1, are < 48% and < 13% respectively. For the estimated linear birefringence, from the corresponding DGD values, this error is further increased due to neglecting the wavelength dependence of the geometrical mode factor, as discussed in Section 5.3, and as we will review in Chapter 7. The error in the measured dispersion values of the stress-optic coefficient in Table 6.1 is expected to be small, due to using a best fit for the slope of the dispersion caused by the circular birefringence (< 10%). Comparing our measured dispersion of the stress-optic coefficient for the S-SMF with e.g. the one measured in Reference [84] of $\omega/g\ dg/d\omega = 0.103$ measured at 1.3 μm, shows good agreement.

Figure 6.21 shows a plot of all the measured DGD values at zero twist for the different fibre types and mirrors the range of DGD values which would be expected in short lengths of fibres, for the corresponding fibre type.

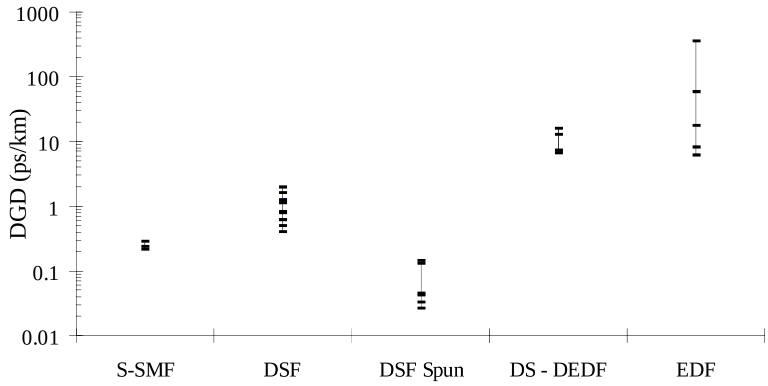

Figure 6.21 Measured DGD values for different fibre types at zero twist

6.4.2 PMD and expected polarisation mode coupling lengths in tension wound fibre bobbins and cabled fibres

6.4.2.1 Expected PMD in spooled fibres

In Figure 6.22(a) the measured short length DGD, of the free-hanging fibre, at zero twist, has been plotted versus wavelength for S-SMF 2 and DSF 3. For Figure 6.22(b) the DGD has been measured on the original shipping bobbins (diameter ~ 15 cm) and plotted versus wavelength for the fibres S-SMF 2 and DSF 1, from which we have measured above the short length DGD. Comparing Figure 6.22 (a) with (b) the DGD reduction due to the random mode coupling seemed to be more effective on the DSF, which has the higher linear birefringence and intrinsic DGD, than on the S-SMF. The strength of the random mode coupling which originates from kinks of the fibre on the bobbin, depends on the winding tension, but winding under tension also induces a certain level of birefringence [78]. For DSFs, an increase in winding tension seems in general to reduce the PMD in the fibre [12], [173], [174], whereas for spun fibre with virtually zero internal PMD, an increase in winding tension seems to increase the fibre PMD due to the additional bending birefringence under tension [12].

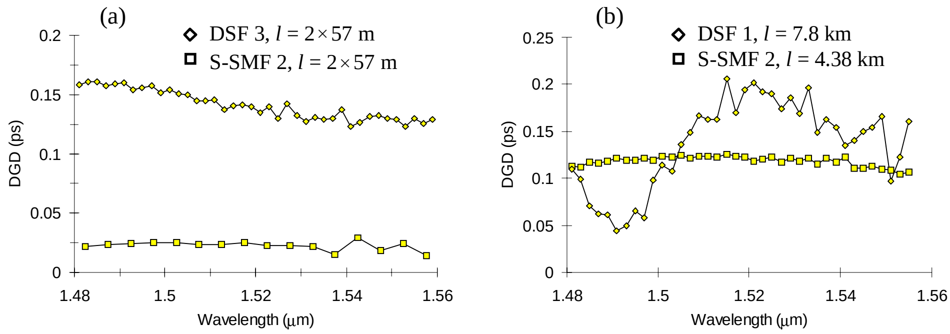

Figure 6.22 Measured DGD versus wavelength, in (a) for S-SMF and DSF fibre at zero twist (free-hanging), and in (b) for S-SMF and DSF on shipping bobbin.

In Figure 6.23 the measured PMD of some of the fibres in Table 6.1 on their shipping bobbins has been plotted versus their measured short length DGD values. The fibre lengths were all > 2.5 km on the bobbins. It can be seen that the measured PMD of the S-SMF, DSFs and spun DSFs on their shipping bobbins show nearly the same value of around 0.04 $ps/\sqrt{km}$, and only the DEDFs seem to reflect their high intrinsic DGD value. Using Equation (6.1) the expected polarisation mode coupling lengths for the DSFs and DEDFs on the fibre bobbin have been calculated to be between 0.1 and 5 metre, which agrees with Reference [97]. In general, we may write down the expected polarisation mode coupling lengths for these kind of fibres as being between 0.1 m < L_C < 10 m if spooled on fibre bobbins. It should be realised that in normalising the measured PMD to the fibre square root length, as carried out in Figure 6.23, we assumed sufficient mode coupling in the measured fibre lengths so that we are in the regime where the PMD increases with the square root of the length. It is also interesting to note that the PMD of the spooled spun fibre shows about the same PMD as for the DSFs due to the bending under tension, which acts as a source of birefringence, rather than promoting efficient random mode coupling on the spun fibre.

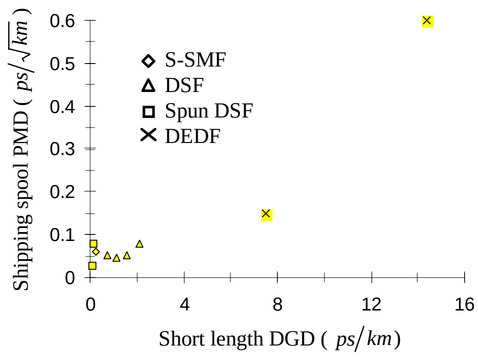

Figure 6.23 PMD on shipping bobbins versus short length DGD for some of the fibres in Table 6.1.

6.4.2.2 *Expected PMD in cabled fibres*

Of more importance than the PMD of the fibre on bobbin is the prediction of the PMD of the cabled fibre as installed under field conditions, which makes it necessary to understand the cabling effect on fibre PMD. The PMD of cabled fibre depends on the cable design, e.g. a loose tube structure which does not induce stress on the fibre, or a structure where the fibre in the package is kept in position, such as tight buffered packages or ribbon cables which can induce stress on to the fibre [12], [66] (see also Subsection 6.15). In general it seems that all the cable designs show an increase in PMD compared to the PMD on the fibre bobbin due to larger polarisation mode coupling lengths in the cables, except for the spun fibre using the loose cable design [12], [175]. The spun fibre, as expected, also shows the lowest sensitivity to temperature changes in its PMD value using the loose structure cable design [13] (see also Subsection 3.3.5). The expected polarisation mode coupling lengths in straight lengths of unspun fibre or in fibres using the loose cable design, has been found to be of the order of a few hundred metres, 100 m < L_C < 500 m, by cut-back method [12], and in measuring the long length PMD and short length DGD of the same cabled fibre [97]. PMD reduction in unspun fibre has also been shown by twisting the fibre prior to cabling which showed PMD reduction compared to untwisted fibres in the final cable [12]. For the tight buffered cable design the design has been modified to obtain a low stress condition for the embedded fibre [12], so that minimum additional external PMD is induced into the fibre by the package, especially for the case if using spun fibre.

Because random mode coupling caused by random perturbing birefringences (e.g. caused by microbends, splice, twist, or stresses induced by the cable) is sensitive to the fibre environment (e.g. ambient temperature), it is not possible to write down a general deterministic relationship between the short length DGD and long length PMD values of a fibre. However, for long lengths of cabled DSFs we may write down the expected range of PMD values from the short length DGD and expected polarisation mode coupling lengths as given above for the loose cable design, by using Equation (6.1). In Table 6.1 the smallest intrinsic DGD value of the measured DSFs is 0.76 ps/km. A long link formed from this fibre is then likely to have a PMD lying in the range $0.2 \rightarrow 0.6 \; ps/\sqrt{km}$. For TAT12 the allowed maximum PMD is 0.15 $ps/\sqrt{km}$ [12], which makes it clear why the fibre used in TAT12 had to be dispersion shifted spun fibre. In general from the above, we may conclude that PMD may be estimated from the short length DGD in (ps/km), by knowing the range of expected polarisation mode coupling lengths in the cabled fibre, but also that measuring the final cable in the factory on a large drum or straight line gives the best prediction of the expected PMD value under field conditions.

6.5 An estimation on bandwidth limitation due to PMD in present and future fibre systems

In this section we will compare the system impairment caused by chromatic dispersion with that caused by first order polarisation mode dispersion. The system degradations due to PDL, PDG, non-linear effects and second order PMD have been neglected in the following discussion, but minimising of the first three impairments has been discussed in Subsection 1.2.4. For more detailed treatment of PDL, PDG and non-linear effects on system performance see also Reference [46].

6.5.1 Bandwidth limitations caused by chromatic dispersion

The theoretical dispersion limit (1 dB optical eye closure penalty) for IM-DD systems using external modulation due to chromatic dispersion, *D* (Equation 3.12), corresponds to a ~25% broadening of the initial pulse and the maximum length, *l*, versus bit-rate, can be estimated by [176], [177]

$$lB^2 D \leq 0.252 \frac{\pi c}{\lambda^2} \approx 10^5 \frac{\left(Gbit/s\right)^2 ps}{nm} \tag{6.7}$$

where *B* is the bit-rate In Figure 6.24(a) the maximum distance as a function of the bit-rate for different chromatic dispersion values is plotted using Equation (6.7). The chosen dispersion values represent the expected dispersion at 1.55 μm for S-SMFs with D = 17 ps/nm•km, DSFs or dispersion compensated S-SMFs with a dispersion in the range of $0.2 < D < 2$. The dispersion limit of S-SMF at 1.55 μm for 10 Gbit/s transmission of non-chirped signals in absence of PMD and non-linearities, is of the order of 60 km, as indicated in Figure 6.24(a). However, chromatic dispersion has now been essentially overcome using DSFs together or dispersion management schemes [5] (Subsection 3.2.3), so that PMD has to be considered [46].

6.5.2 First order PMD induced bandwidth limitations

The DGD ($\Delta\tau$) originating from the intrinsic birefringence is a statistical variable due to the random birefringent perturbations along the fibre, which may change with time due to local fluctuations of temperature or stress [9], [126], [144], and is best described by a Maxwellian distribution as shown in Figure 3.21 [130]. The random variation of $\Delta\tau$ can be also described by the random variation of the output SOP and PSPs with time, which for a fixed input SOP results in a random shifting of power between the two PSPs.

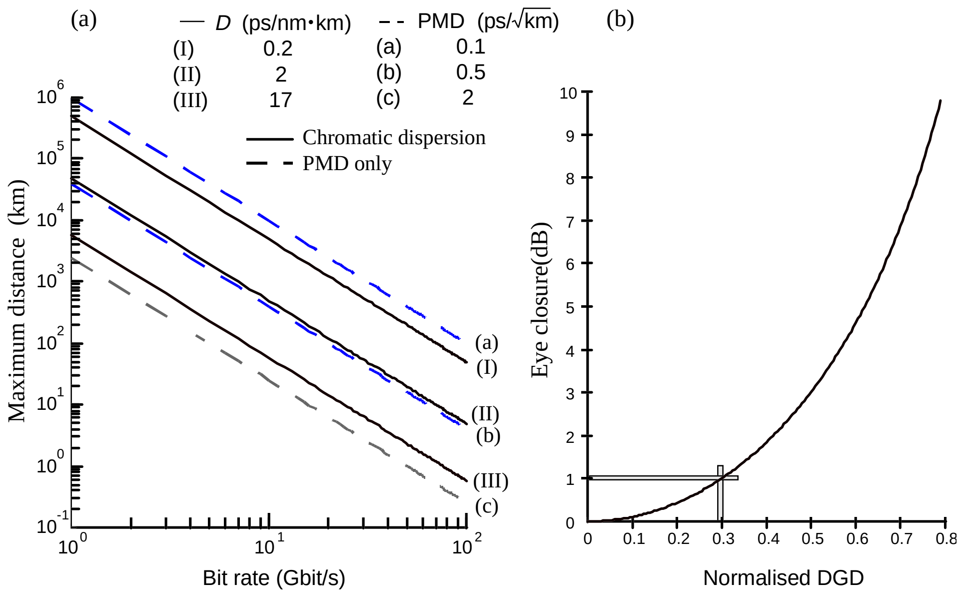

Figure 6.24 Transmission limitation at 1.55 μm for single channel chirp free NRZ signal in non-regenerated optical system. In (a) due to chromatic dispersion and for PMD. In (b) electrical eye closure as a function of the normalised DGD (From [46]).

PMD, unlike PDL and PDG causes a bit-rate dependent penalty on transmission, causing ISI, which can be measured with the eye closure [9], Q-factor [178], and BER [179], [180]. It has been identified that for an allowed 1 dB sensitivity penalty (path penalty allocated to PMD), the *normalised DGD* = $\Delta\tau \bullet B$ should be limited to 30% of the bit period as shown in Figure 6.24(b). Furthermore, given the Maxwellian distribution of PMD, the bit period "budget" must be further reduced to protect the system against some low probability excursion into the tail of the distribution. A safety factor of three times the mean value protects against a ~10^{-5} probability excursion in the Maxwellian distribution, as shown in Figure 6.25(a), and has been suggested for terrestrial systems [181], [182], whereas for submarine systems this factor is sometimes 4.2 (see Figure 6.25(a)), for the higher reliability required of these systems [183]. Therefore, for terrestrial systems the provisionally allowed bit period 'budget' is 10% (0.3/3) of the mean value of the DGD. Constraining the mean DGD (PMD) of a link to a 10% of the bit period, the maximum system length *l* (km) for a given PMD and bit-rate *B* is given by

$$l = \frac{10^4}{B^2 \cdot PMD^2} \; km \tag{6.8}$$

where the PMD and B co-efficients are in their usual units ($ps/\sqrt{km}$ and Gbit/s). The maximum distance for PMD limited transmission using Equation (6.8) is plotted in Figure 6.24(a) together with the chromatic dispersion as a function of bit-rate, for some typical minimum to maximum PMD values, as may be expected in some networks (see Appendix B). The higher the bit-rate, the more drastic the PMD induced penalty becomes, and the maximum non-regenerated fibre span scales inversely with B^2 as for the chromatic dispersion. In Figure 6.25(b) the maximum PMD limited transmission has been directly plotted versus PMD for the bit-rates 5, 10 and 20 Gbit/s, indicating also the expected PMD range of cabled S-SMFs, DSFs and spun DSFs. The expected PMD range for the cabled DSFs has been estimated from the measured DGD values given in Table 6.1 using Equation (6.1) with the polarisation mode coupling lengths for cabled fibres as given in Subsection 6.4.2.2, whereas for the S-SMF and spun DSF the typical PMD range has been gathered from external sources, as for example [182], [184]-[186] (see Appendix B).

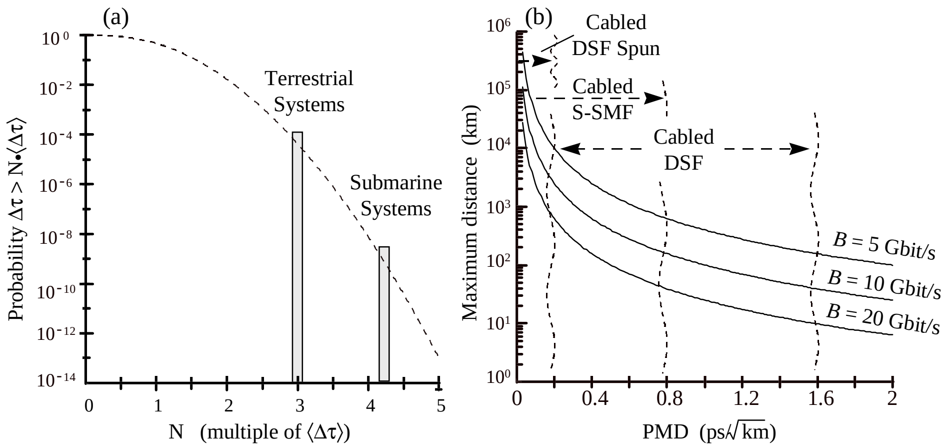

Figure 6.25 In (a) probability density function of N times the mean DGD value ⟨Δτ⟩, and in (b) the maximum distance limit due to PMD for a 5, 10 and 20 Gbit/s NRZ signal.

For example, in a terrestrial system operating at 5 Gbit/s, PMD values of the order of $2\,ps/\sqrt{km}$ would be a threat for the uncompensated S-SMF for distance > ~ 60 km, as can be seen in Figure 6.24(a). Moreover, it can be seen that when up-grading systems to bit-rates

> 10 Gbit/s by using dispersion compensation techniques the maximum PMD over distances ~200 km should be smaller than $0.7\ ps/\sqrt{km}$.

For optically amplified submarine systems like TAT12, we use the suggested safety factor of 4.2 times the mean DGD value, which yields an allowed bit period ‘budget’ of ~7% (0.3/4.2). We note that TAT 12/13 is designed for 5 Gbit/s operation with a single wavelength at the effective zero chromatic dispersion using spun DSF with dispersion compensating fibre (DCF) in each span. The design figure taken for the TAT12 link allowed a maximum PMD of $0.15\ ps/\sqrt{km}$ [12], which would result in a total PMD time of 12 ps over the 6400 km length, which in turn is 6% of the bit period. For properly cabled spun fibres the PMD can be expected to be ~ $0.1\ ps/\sqrt{km}$ [12], which for a 10 Gbit/s transatlantic system working at a single frequency would result in a ~ 1.3 dB penalty.

With the commercial availability of 10 Gbit/s TDM systems coupled with external modulation and dispersion compensation techniques, operators of terrestrial networks have performed PMD measurement intensively in their networks [100], [182], [184]-[186], over the last few years, to ensure reliability for future upgrading of the network capacity to higher bit-rates. In Appendix B, a review on reported PMD values measured in installed systems (mainly S-SMF) from different network operators across Europe is provided. The majority of these reported PMD values lie between ~ 0.01 and 0.8 $ps/\sqrt{km}$ (see also Figure 6.25(b)), indicating the expected PMD range for cabled S-SMF) which for the higher one would limit the maximum distance to ~160 km (see Figure 6.25(b)). It seems to be that in up-grading the majority of installed fibres (cables) to 10 Gbit/s TDM systems, no large problem due to PMD may be expected. However, PMD still remains an issue for some links which show unacceptably high PMD values for 10 Gbit/s TDM transmission (depending on the country, see Appendix B).